

2
3
4 **Potential for Perceived Failure of Stratospheric Aerosol**
5 **Injection Deployment**

6
7 Patrick W. Keys^{1,2*}, Elizabeth A. Barnes¹, Noah S. Diffenbaugh³, James W. Hurrell¹ and Curtis M. Bell⁴

8
9 ¹ Department of Atmospheric Science, Colorado State University

10 ² School of Global Environmental Sustainability, Colorado State University

11 ³ Doerr School of Sustainability, Stanford University

12 ⁴ International Programs Department, United States Naval War College

13
14
15 ***Corresponding Author:** Patrick W. Keys

16 **Email:** patrick.keys@colostate.edu

17
18 **Author Contributions:** PWK and EAB conceived the study; EAB developed the code; PWK, EAB and
19 NSD designed and conducted the analysis; EAB, PWK and NSD created the figures; all authors
20 contributed to writing the paper.

21 **Funding:** Work was supported by the Defense Advanced Research Projects Agency #HR00112290071
22 (PWK, EAB and JWH), the LAD Climate Fund (JWH) and Stanford University (NSD).

23 **Acknowledgements:** The views expressed here do not necessarily reflect the positions of the U.S. Naval
24 War College and the United States government.

25 **Keywords:** climate change; internal climate variability; solar geoengineering; perception; mitigation

26

27 **Abstract**

28 As anthropogenic activities warm the Earth, the fundamental solution of reducing greenhouse gas
29 emissions remains elusive. Given this mitigation gap, global warming may lead to intolerable climate
30 changes as adaptive capacity is exceeded. Thus, there is emerging interest in solar radiation modification,
31 which is the process of deliberately increasing Earth's albedo to cool the planet. Stratospheric aerosol
32 injection (SAI) — the theoretical deployment of particles in the stratosphere to enhance reflection of
33 incoming solar radiation — is one strategy to slow, pause or reverse global warming. If SAI is ever
34 pursued it will likely be for a specific aim, such as affording time to implement mitigation strategies,
35 lessening extremes, or reducing the odds of reaching a biogeophysical tipping point. Using an ensemble
36 climate model experiment that simulates the deployment of SAI in the context of an intermediate
37 greenhouse gas trajectory, we quantify the probability that internal climate variability masks the
38 effectiveness of SAI deployment on regional temperatures. We find that, while global temperature is
39 stabilized, substantial land areas continue to experience warming. For example, in the SAI scenario we
40 explore, up to 55% of the global population experiences rising temperatures over the decade following
41 SAI deployment, and large areas exhibit high probability of extremely hot years. These conditions could
42 cause SAI to be perceived as a failure. Countries with the largest economies experience some of the
43 largest probabilities of this perceived failure. The potential for perceived failure could therefore have
44 major implications for policy decisions in the years immediately following SAI deployment.

45

46

47

48 **Significance Statement**

49 Even if aggressive mitigation policies are implemented soon, climate change impacts will worsen in the
50 coming decades. One proposed response is stratospheric aerosol injection (SAI), which would reflect a
51 small amount of the sun's energy back to space, thereby cooling the planet. This approach is broadly
52 considered to be relatively inexpensive and straightforward to deploy, and global cooling could occur
53 rapidly. However, on regional scales, internal climate variability is likely to dominate over SAI forcing.
54 This means that in the decade after SAI is deployed, many regions of the world could locally experience
55 even higher temperatures. Our study provides conceptual insight for the possible perception of failure of
56 SAI, or other climate mitigation strategies.

57 **Introduction**

58

59 Anthropogenic climate change, primarily driven by increasing concentrations of atmospheric greenhouse
60 gasses, has caused Earth’s global mean temperature to reach its warmest level in at least the last 2,000
61 years (1). This global warming may exceed 1.5°C above pre-industrial temperatures later this decade, at
62 least for a short-period of time, and most years are likely to exceed the 1.5°C threshold by 2040 across a
63 range of emissions scenarios (IPCC 2021). By the middle of this century (2041-2060), warming in excess
64 of 2.0°C would be reached under intermediate, high and very high emission scenarios (1), and current
65 policies have the world on track to warm by roughly 3.0°C by the end of the century (2). Moreover,
66 emissions scenarios that target global temperature stabilization at either 1.5 or 2.0°C require net-zero
67 carbon emissions trajectories, which in practice will necessitate new and enormously-scaled-up carbon
68 dioxide removal technology (3).

69

70 In parallel with global policy shortfalls, current levels of warming are driving substantial impacts on
71 human and natural systems (IPCC 2022). For example, climate change is already leading to
72 intensification of extreme events such as extreme heat, heavy rainfall, intense droughts, extreme wildfire
73 weather and marine heatwaves (4). These and other climate changes are leading to a broad suite of
74 impacts, such as migration of ecological niches (5), increases in global tree mortality (6), increases in
75 financial losses from extremes (e.g., 7), and amplification of existing economic inequality (8) and social
76 injustices (9). Furthermore, there is the possibility that biogeophysical tipping points may lead to new
77 states in key Earth systems, such as irreversible Antarctic ice loss, tropical rainforest dieback, and slowing
78 ocean circulations (10). These so-called tipping points are highly uncertain — in terms of whether, when,
79 and how they may occur (1). Despite this uncertainty, there is paleoclimate evidence that tipping points
80 have been crossed in the past, and emerging evidence suggests that they could be crossed as a result of
81 anthropogenic change (11–13).

82

83 To possibly grant humanity additional time to sufficiently reduce greenhouse gas emissions, lessen the
84 existing negative impacts of climate change, and avoid transgression of irreversible tipping points, there is
85 renewed interest in developing an international research agenda on solar radiation modification (SRM) —
86 a speculative form of climate change response that has the potential to offset human-induced warming by
87 reflecting a small amount of solar energy back to space before it enters and warms the planetary
88 environment (14).

89

90 There are numerous challenges for advancing SRM science and research. First, there are substantial
91 ethical questions concerned with committing future generations to an uncertain technology and the
92 potential burden of continuing climate intervention well into the future (15) or deciding when and how to
93 ramp down SRM deployment (16–19). Second, there are important concerns related to how climate
94 intervention may drive changes in essential Earth system processes (20, 21). Third, there are concerns that
95 the negative consequences arising from SRM would disproportionately burden populations that are
96 systematically already burdened by climate change impacts, global dispossession of resources, and wealth
97 inequality (22, 23). Research investigating public opinion has found considerable heterogeneity in
98 attitudes toward either research or use of climate intervention (24).

99
100 In addition to these social challenges, there exist basic scientific questions about how to distinguish the
101 climate effects of SRM from anomalies driven by internal variability of the Earth system (25, 26). This
102 variability can lead to substantial short-term variation in socially-relevant climate phenomena, such as the
103 frequency of extreme hot and cold spells (27), the severity of drought (28), the path of the midlatitude
104 storm tracks (29), changes in regional temperature and precipitation (30), the state of Arctic sea ice (31),
105 or the strength of tropical modes of variability such as the El Niño Southern Oscillation (32) or the
106 Madden-Julian Oscillation (33). Research on the interaction between human-induced climate impacts, or
107 “signals”, and internal climate variability, or “noise”, is a critical area of climate change science, not least
108 for supporting policymakers and the public in navigating the expectations of climate change action
109 against a backdrop of an internally-varying climate system (34).

110
111 Stratospheric aerosol injection (SAI) is the SRM strategy of releasing particles into the stratosphere to
112 slow, pause, or reverse global warming (35). While climate simulations provide evidence that the long-
113 term result of SAI could lead to stabilized global temperatures (17), the impacts of SAI may be regionally
114 heterogeneous with temperature and precipitation varying considerably (36–39). Moreover, internal
115 climatic variability may mask the short-term perceived effectiveness of SAI. That is, it is possible that
116 while SAI could successfully stabilize mean global temperatures, the perceived effectiveness on *regional*
117 scales may be overwhelmed by local climatic variability over the short term. Psychologically, a climate
118 change-related event connects to people’s perceptions most clearly when it is directly and locally relevant
119 (40, 41). Moreover, people who are residents of a specific location may tacitly incorporate 10-year trends
120 in their perception of changes in climate (42). Hence, local changes in climate – such as continued
121 warming or the occurrence of extreme events – may cause climate interventions such as SAI to be
122 perceived as a failure. Given the potential for SAI to abruptly cease, and the likelihood of rapid climate
123 change following such cessation (e.g., 19, 43, 44), the perception of failure carries particular risks.

124
125 If SRM is ever pursued, it will likely be for a specific social or geophysical aim (22). This may include
126 halting an anticipated geophysical tipping point (such as accelerated Antarctic ice loss (45) permafrost
127 melting or forest die-off), or lessening the impacts of extremes (such as deadly heat waves in large
128 population centers (46)). Yet, if climate variability were to mask the short-term perceived effectiveness of
129 climate intervention, it could undermine coordinated, international policy action to address climate
130 change broadly (47). Understanding the masking effects of climate variability on regional scales will thus
131 be critical for interpreting the potential perceived success of any SRM strategy in the immediate years
132 following deployment.

133
134 To systematically distinguish the different possible outcomes associated with the masking effect of
135 internal climate variability, we introduce a set of archetypal regional responses that could unfold under
136 SAI. These archetypes are motivated by the fact that, in the period prior to SAI deployment, a given
137 region could be warming or not due to internal climate variability, even in the context of global-scale
138 warming (48). Similarly, following deployment, that region could either experience warming or not, even
139 if the global temperature is stabilized. Thus, we define four archetypes of perceived success of climate
140 intervention, based on four categories of pre- and post-deployment experience: 1) Rebound Warming (i.e.
141 no warming followed by warming); 2) Continued Warming (i.e. warming followed by more warming); 3)
142 Stabilization (i.e. no warming either before or after deployment); and, 4) Recovery (i.e. warming followed
143 by no warming). The phenomena “Rebound Warming” and “Continued Warming” could both be locally
144 perceived as a failure of SAI to deliver on its intended purpose; hence, throughout the rest of this work,
145 the phrase ‘perceived failure’ refers to the combination of these two archetypes.

146
147 Past research into global SRM strategies has employed climate or Earth system models to simulate how
148 the natural system may respond to different intervention approaches (49). Here, we leverage just one of
149 them: the Assessing Responses and Impacts of SRM on the Earth system with Stratospheric Aerosol
150 Injection (ARISE-SAI) ensemble carried out with the Community Earth System Model, version 2 (50).
151 ARISE-SAI simulates a plausible deployment of SAI, designed to hold global mean temperature at 1.5°C
152 above pre-industrial conditions in the context of the SSP2-4.5 future emissions scenario (Fig. 1A) (50).
153 Extending out to the year 2069, ARISE-SAI includes 10 ensemble members, each initiated from slightly
154 different initial conditions to enable quantification of the irreducible uncertainty arising from internal
155 climate variability (e.g., 51). The 1.5°C threshold is relevant for global policy discourse in part because
156 this is a global mean temperature increase that is considered both an important Earth system threshold, as
157 well as a key focus of global climate policy negotiations enshrined in the UN Paris Agreement (52). The

158 fact that ARISE-SAI simulates SAI deployment that stabilizes global temperature at 1.5°C while also
159 representing the effect of internal variability via a substantial number of ensemble members makes
160 ARISE-SAI a useful testbed for probing the possibility of perceived failure of climate intervention.

161

162 **Results**

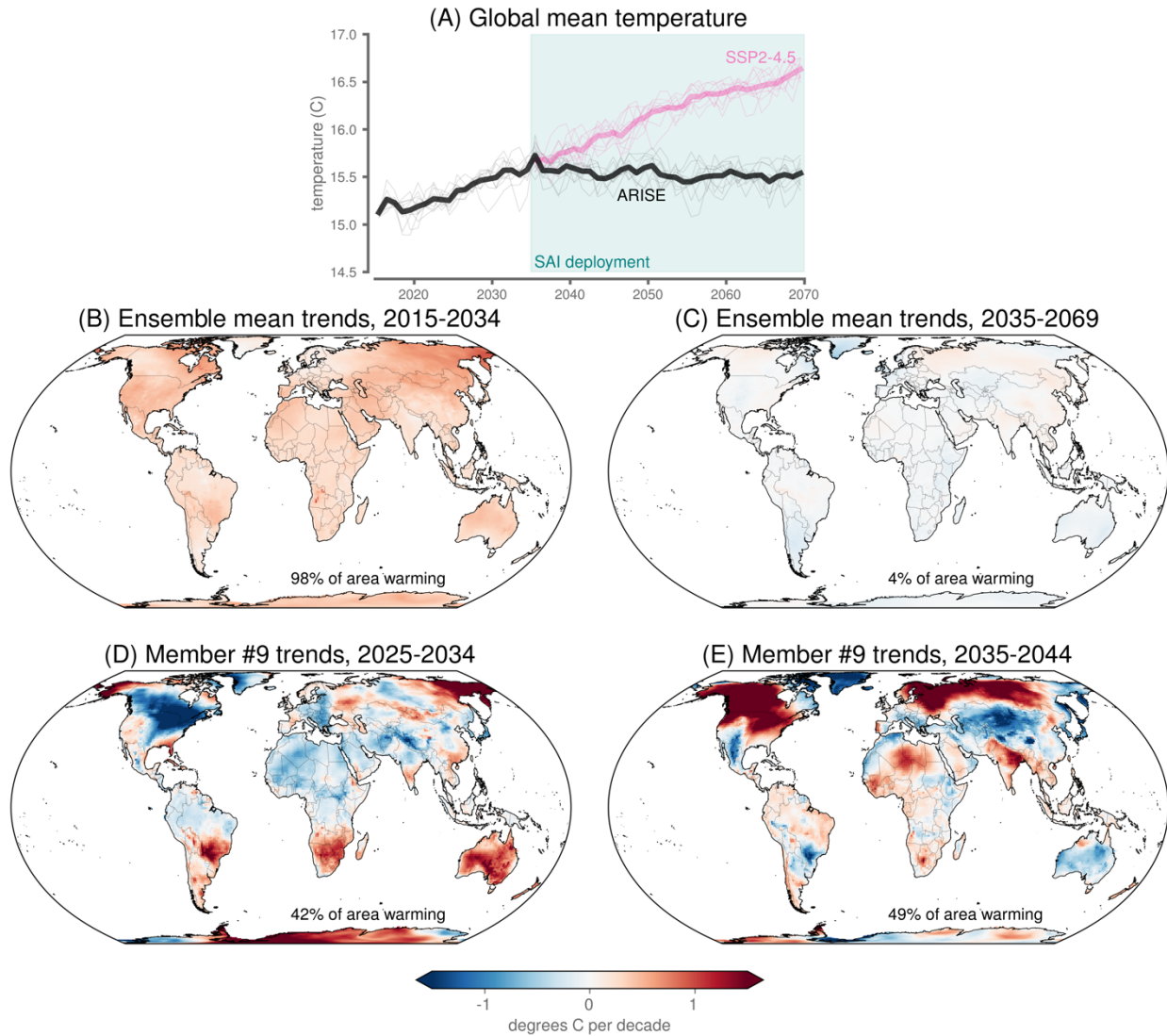
163

164 Increases in greenhouse gas concentrations and other anthropogenic forcings under the SSP2-4.5 scenario
165 drive increases in temperatures globally (Fig. 1A), as seen in the forced (ensemble-mean) response during
166 the 2015-2034 pre-deployment period of ARISE-SAI (Fig. 1B). Visualizing the ensemble mean reduces
167 many of the effects of internal climate variability, even though an ensemble of more than 10 members is
168 likely needed to fully remove such effects regionally (e.g., 48, 53). Over the longer post-deployment
169 period of 2035-2069, the ensemble mean exhibits a clear picture of temperatures generally holding steady
170 throughout the rest of the simulation (Fig. 1A), indicative of SAI acting to stabilize temperatures even
171 regionally (Fig. 1C). In reality, however, any area’s actual climate trajectory will be a combination of
172 both the forced response and internal climate variability, which would be analogous to a single ensemble
173 member (Fig. 1D,E) rather than the ensemble mean.

174

175 Focusing on the decade prior to SAI deployment (“pre-deployment decade”; 2025-2034), any ensemble
176 member (e.g. member #9) will exhibit a large range of temperature trends regionally under SSP2-4.5 (Fig.
177 1D), even though the forced response is overwhelmingly warming. This is because internal climate
178 variability can drive short-term trends in temperature that can partially mask (or augment) the longer-
179 term, forced trend. What is perhaps less appreciated is that internal climate variability can similarly mask
180 the effects of SAI on a regional scale. In the decade following continuous SAI deployment (“post-
181 deployment decade”; 2035-2044), ensemble member #9 exhibits warming temperatures over 49% of the
182 land surface (Fig. 1E), where warming is defined as decadal temperature trends larger than 0.1 °C/decade.
183 This trend threshold is chosen to reflect the approximate warming over the observational record (54);
184 temperature trends less than this are referred to here as ‘not warming’ since they capture both cooling as
185 well as small positive trends. Thus, the effects of internal climate variability can cause the magnitude of
186 regional warming trends in the post-deployment decade to far exceed the forced trend from SAI.

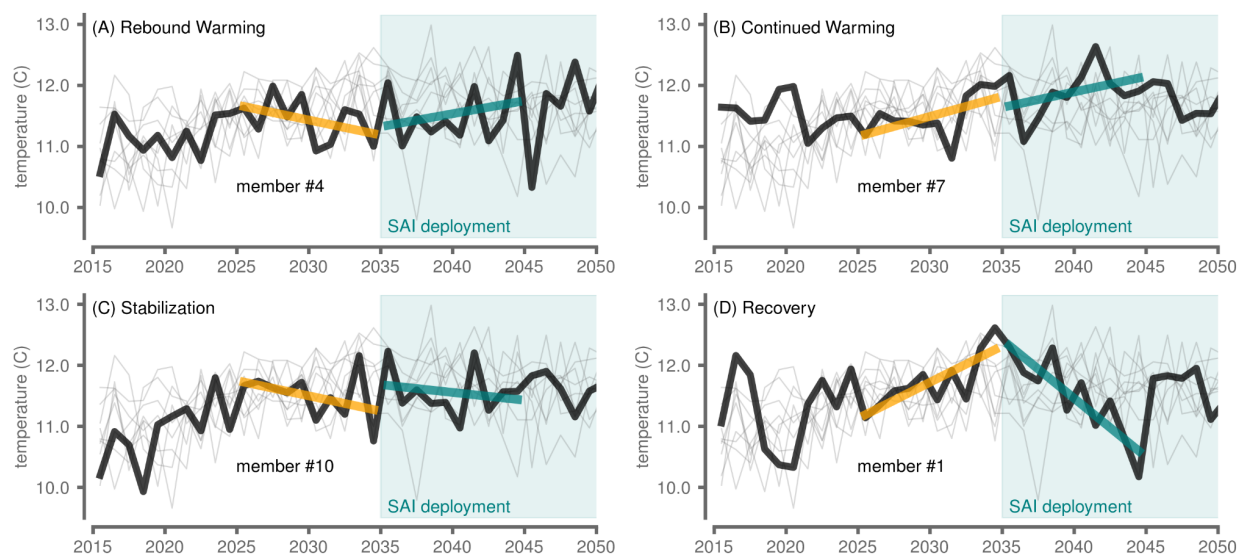
187



188
 189
 190
 191
 192
 193
 194
 195

Figure 1. Surface temperature trends. (A) Global mean surface temperature. Gray lines denote individual ensemble members and the black line denotes the ensemble mean. (B,C) Ensemble-mean trends over (B) 2015-2034 under SSP2-4.5 and (C) 2035-2069 with ARISE-SAI deployment. (D,E) Trends over the (D) pre-deployment decade and (E) post-deployment decade for ensemble member #9. (B-D) The percentage in the bottom of the maps denotes the percentage of land area that exhibits warming trends as defined in the text.

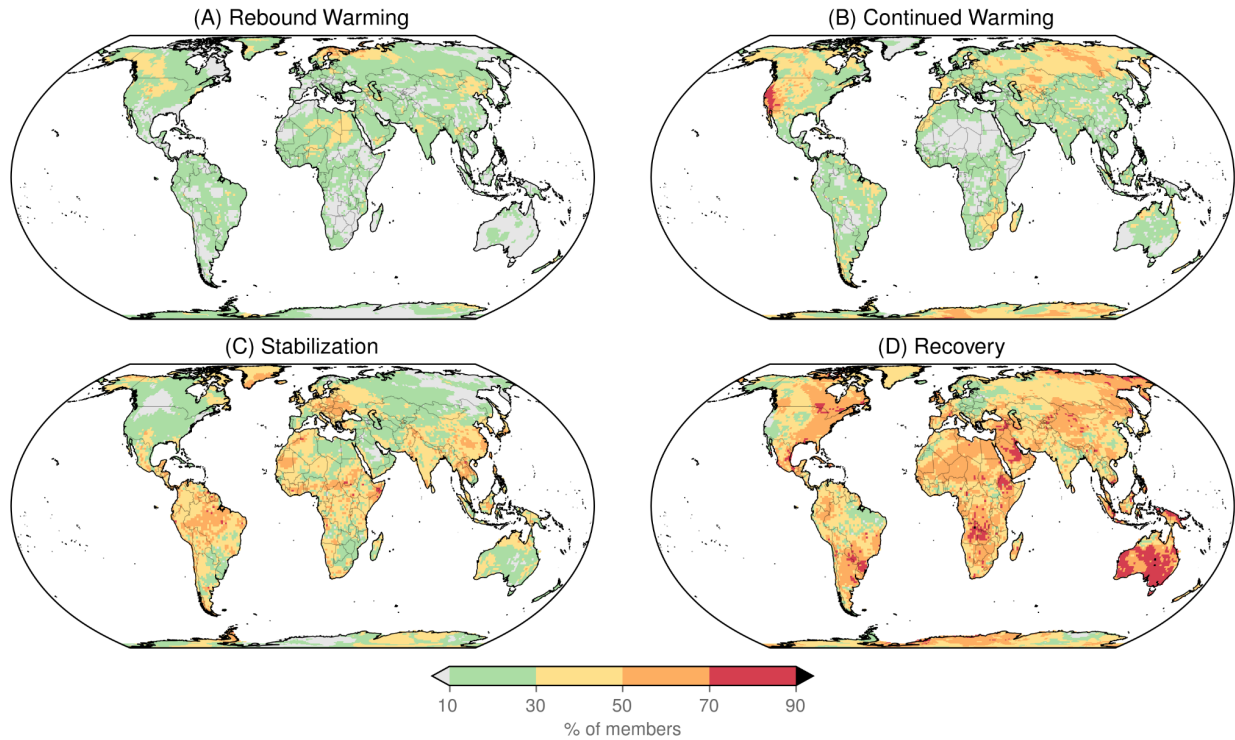
Beijing, China



196
197 **Figure 2.** Pre-deployment and post-deployment surface temperature trends for Beijing, China. Each panel highlights
198 a different ensemble member denoted in each panel by the thick black line, with the other nine members shown as
199 thin gray lines. SAI deployment is initiated in the year 2035 (teal shading). Ten-year linear best-fit lines are shown
200 for 2025-2034 (orange) and 2035-2044 (teal).

201
202
203 Beijing, China, provides an example of how a single region can experience each of the four archetypal
204 responses under different individual realizations of the ARISE-SAI experiment (Fig 2). Ensemble
205 member #1 exhibits the Recovery archetype (Fig 2D), where SAI would potentially be labeled a success
206 in that the perception of temperature change would swing from an increase in local temperature prior to
207 deployment to a stabilization or decrease in temperature after deployment. However, in member #4,
208 Beijing experiences Rebound Warming (Fig 2A), with cooling over the pre-deployment period followed
209 by warming over the post-deployment period. Likewise, in member #7, Beijing experiences Continued
210 Warming (Fig 2B), with substantial warming during both the pre- and post-deployment decades.

211
212



213
 214 **Figure 3.** Archetypal regional responses to ARISE-SAI. The percent of ensemble members that exhibit specific
 215 archetypal responses over the ten years pre- and post-deployment: (A) Rebound Warming (not warming followed by
 216 warming), (B) Continued Warming (warming followed by warming), (C) Stabilization (not warming followed by
 217 not warming) and (D) Recovery (warming followed by not warming).

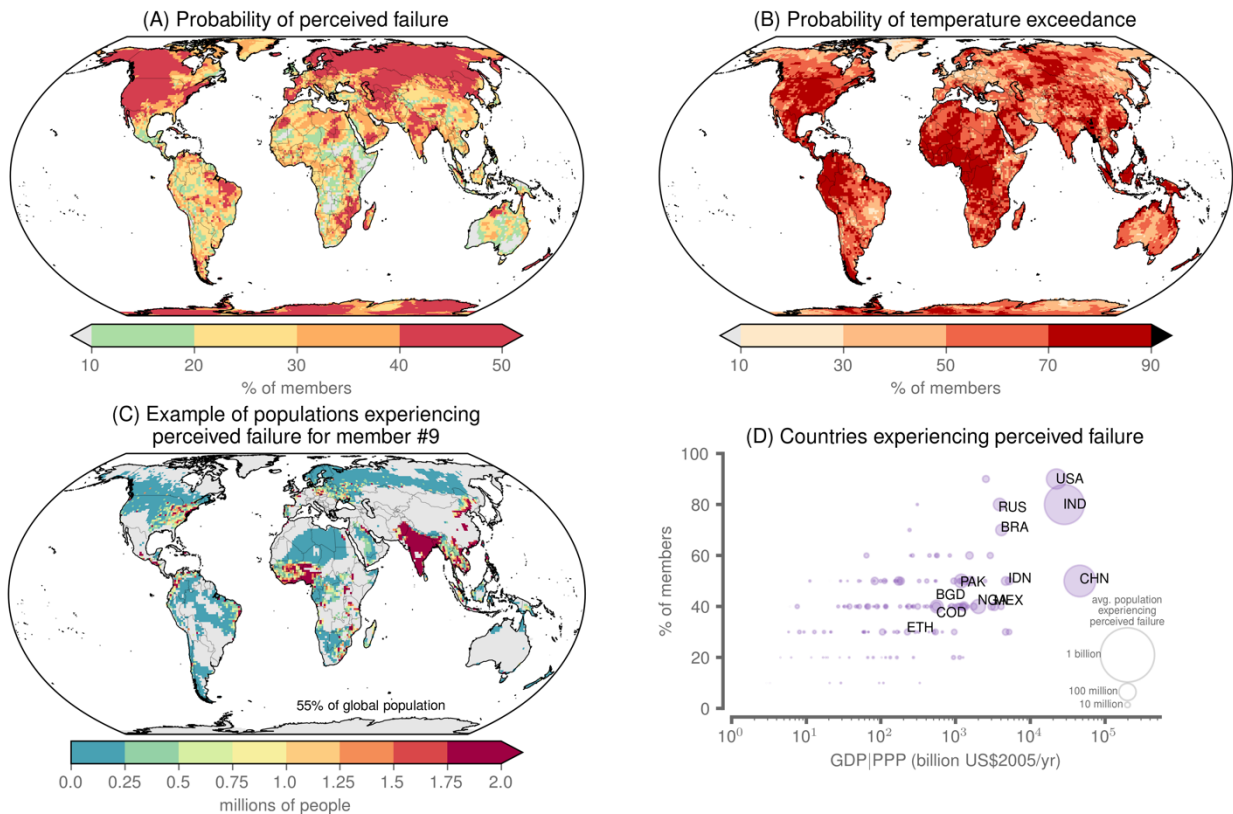
218
 219
 220 All four archetypal regional responses can be found across the globe, with varying percentages of the
 221 ARISE-SAI ensemble (Fig 3). While some regions, notably Australia and parts of Africa, exhibit high
 222 probability of the Recovery archetype (Fig 3D), substantial parts of the land surface experience high
 223 probability of either Rebound Warming or Continued Warming. Repeated occurrence of perceived failure
 224 in the same location across multiple ensemble members can be largely understood as internal climate
 225 variability persistently masking the effect of SAI deployment (although more than ten ensemble members
 226 would be required to completely rule out the possibility of a weak, short-term forced response to SAI
 227 itself; Fig. 1C).

228
 229 Aggregating the occurrence of Rebound Warming and Continued Warming across all ensemble members
 230 yields the probability (computed as the percent of the 10 ensemble members) of internal variability
 231 leading to perceived failure of SAI in the ARISE-SAI experiment (Fig 4A and 4B). While some regions
 232 of the planet experience near-zero probability of perceived failure under ARISE-SAI deployment, there

233 are other regions that experience greater than 50% probability of perceived failure. East Antarctica — a
 234 region of global importance and priority with respect to the potential for substantial changes in sea level
 235 (55) — appears particularly prone to climate variability masking the effectiveness of climate intervention.
 236 Likewise, much of northern Eurasia and the western half of North America experience a very high
 237 probability of perceived failure in the decade following deployment. For the case of North America,
 238 Pacific Decadal Variability – which CESM is known to simulate with high fidelity (56) – could be a key
 239 factor confounding the effects of climate intervention (Fig. S3).

240
 241 We emphasize that these results are specific to the ARISE-SAI deployment, which is only one of many
 242 possible SAI deployment scenarios (e.g., 57). Regardless, they suggest that internal variability in the
 243 climate system, whether arising from random noise in the atmosphere or oceans (Deser et al. 2017) or
 244 from potentially predictable coupled ocean-atmosphere modes of variability, can effectively mask SAI
 245 deployment.

246
 247



248
 249 **Figure 4.** Perceived failure over the ten years following SAI deployment under ARISE. (A) Probability of perceived
 250 failure over the post-deployment period, where the probability is computed as the fraction of ensemble members
 251 exhibiting warming trends. (B) Probability of a location exceeding its 2015-2034 (pre-deployment) maximum

252 annual-mean temperature in the decade following SAI deployment (2035-2046). (C) Projected number of people at
253 each location experiencing perceived failure of SAI over the post-deployment period in ensemble member #9 using
254 projected populations for 2040. Gray denotes regions not experiencing perceived failure in that particular ensemble
255 member. (D) Percent of members with 10% or more of a country's projected 2040 population (see Fig S5 for
256 alternative population thresholds) experiencing perceived failure following SAI deployment versus the country's
257 projected 2040 GDP in units of purchasing power parity (PPP). Circle area corresponds to the projected 2040
258 population experiencing perceived failure averaged across ensemble members.

259
260

261 Our perceived failure metric relies on quantifying decadal temperature trends. However, given the myriad
262 impacts of extreme heat on natural and human systems [\(27, 58\)](#), an alternative metric for the perceived
263 effectiveness of SAI could instead be a measure of the experience of temperature extremes following
264 deployment. We find that, although the forced response in ARISE-SAI results in a stabilization of global
265 temperatures (Fig. 1A,C), it is still very likely that record hot temperatures will occur following
266 deployment (Fig. 4B). For example, for broad areas of Africa, Eurasia, North America, South America
267 and Antarctica, at least one year in the decade after SAI deployment is hotter than the hottest year that
268 occurred in 2015-2034. Moreover, the regions experiencing persistently high perceived failure of SAI
269 (Fig 4A) do not directly correspond to the regions experiencing extremely high mean annual temperatures
270 (Fig 4B). This finding underlines that multiple climate metrics are necessary when considering the
271 perceived effectiveness of SAI.

272

273 Given the importance of local experiences for informing perceptions of climate change [\(40\)](#), we next
274 explore the populations exposed to perceived failure of SAI in the specific ARISE-SAI deployment
275 scenario examined here. Using gridded population data projected for 2040 in SSP-2 [\(59, 60\)](#), we find that
276 between 10% and 55% of the global population experience perceived failure across the ten-member
277 ARISE-SAI ensemble (Fig S4). The most severe example is shown in Fig 4C for ensemble member #9,
278 where substantial populations in India, Southeast Asia, the Eastern United States, and West Africa are
279 exposed to the potential of perceived failure over the decade following ARISE-SAI deployment.

280

281 Perceptions of climate change-related phenomena can be related to both individual local experiences, as
282 well as collective socio-cultural experiences [\(40, 61, 62\)](#). Thus, to further explore the socio-economic
283 reality of perceived failure of SAI at the national level, we compare the probability of country-level
284 perceived failure against country-level gross domestic product in 2040 (in units of purchasing power
285 parity, PPP) [\(63\)](#). All of the largest economies in the world experience substantial probability of
286 perceived failure in the post-deployment decade of ARISE-SAI (Fig 4D). The implication is that the

287 countries with the most geopolitical and global economic power — and perhaps those with the most
288 financial capacity to deploy continuous SAI to manage global temperatures (64) — experience at least a
289 50% probability of large populations being exposed to the potential of perceived failure of SAI. These
290 countries also cover substantial land areas, potentially increasing the odds that internal climatic variability
291 could mask the benefits of SAI. Yet, the fact remains that the countries that are apparently most prone to
292 high potential of perceived failure are those with the largest populations and the largest economies.

293

294 **Discussion**

295 The ‘fast’ dimension of climate intervention is a notable advantage of SAI relative to other climate
296 intervention approaches (14, 24). However, we find that substantial areas of the world could experience
297 warming trends and extremely hot years, even after ten years of continuous deployment in the ARISE-
298 SAI scenario—raising the possibility that SAI may not be perceived locally as effective. Given the
299 potential social, political and economic costs associated with climate intervention, and increasing stakes
300 associated with a warming planet, this gap in time between deployment and local perceived effectiveness
301 could serve to undermine the ‘fast’ dimension of SAI intervention. Moreover, SAI is a technology that
302 could potentially be deployed quickly by a small group of actors (or a single actor), owing to its relatively
303 low cost and ease of deployment from a single location on the planet (e.g., within the borders of a single
304 country) (35, 64).

305 In light of our findings, several priorities emerge for a forward-thinking SAI research agenda. First, the
306 prevalence of perceived failure suggests countries should expect public doubt in the short-term
307 effectiveness of SAI. The expectation of precise manipulation would be markedly inaccurate (65).
308 Moreover, different types of SAI deployment scenarios could lead to different levels of masking (both
309 more and less) of internal climate variability. However, this issue will also emerge in the midst of more
310 general mitigation efforts (66), as internal climate variability will likely produce continued warming in
311 some regions in the years following aggressive policies aimed at reducing greenhouse gas emissions—
312 potentially leading to similar ‘perceptions of failure’ in the climate policy itself (67). Thus, whether or not
313 SAI is pursued, countries must recognize that internal climate variability will need to be anticipated and
314 well-articulated if continued public support is desired. Furthermore, this articulation must occur amidst a
315 communication environment that is already fraught with climate-related mis-information (68).

316

317 To further explore the relevance of the perceived failure archetypes, we performed a similar analysis
318 using data from the Geoengineering Large-Ensemble SAI experiment (GLENS-SAI; Tilmes et al. 2018).
319 The results provide complementary insights into SAI deployed under a much higher emissions scenario
320 (Representative Concentration Pathway 8.5; RCP8.5) and different stabilization targets and deployment

321 year (deployment in the year 2020 with the main aim to keep global temperatures around 1°C above pre-
322 industrial values). Because of this, GLENS-SAI represents a much more aggressive SAI scenario than
323 ARISE-SAI. The GLENS-SAI results (see Supplementary Materials) again illustrate the regional
324 significance of internal climate variability, and thus further indicate that the potential for perceived failure
325 will exist across many different SAI deployment strategies.

326

327 Given that specific regions of the planet are predisposed to the effects of large internal climate variability,
328 such as that produced by El Niño Southern Oscillation or the Pacific Decadal Oscillation (69), it is likely
329 that these regions will also experience persistent masking of SAI effectiveness. Such understanding of
330 regionally persistent masking of SAI effectiveness will complement and contribute to the growing
331 literature on detection and attribution of deployment of climate intervention (25, 26). Further, because the
332 possibility of perceived failure extends beyond SAI, knowledge of specific regionally persistent internal
333 variability will benefit other climate mitigation policies, especially those contingent on public support
334 (70).

335

336 **Conclusions**

337 Our results highlight the need for continued research and understanding of how climate variability may
338 mask climate intervention in the years immediately following deployment. If climate intervention is ever
339 pursued, it will likely be for a specific social or geophysical aim. Internal climate variability, however,
340 may mask the short-term perceived effectiveness of that intervention, including in the targeted
341 geographical areas, ecosystems or economic sectors for which the intervention was deployed in the first
342 place. Our results thus suggest that the scientific community must better frame what the success of SAI –
343 and climate intervention more broadly – looks like in the context of internal climate variability.

344 Specifically, it will be important to understand how key global drivers of variability, such as coupled
345 ocean-atmosphere modes operating on decadal timescales, may mask the intended results of climate
346 intervention strategies, and to what extent this masking will be predictable or detectable. Our analysis
347 provides a foundation for that understanding, and motivation for improving the ability of global policy
348 and scientific organizations to better frame the stakes associated with the deployment of climate
349 intervention in the future.

350

351 **Methods**

352

353 *ARISE Data*

354 Gridded, monthly near surface air temperature fields (variable name TREFHT) were obtained from the

355 ensemble of simulations performed for the Assessing Responses and Impacts of SRM on the Earth system
356 with Stratospheric Aerosol Injection (ARISE-SAI) (50). The ARISE ensemble was simulated with the
357 Community Earth System Model, version 2 (71) using WACCM6 (Whole Atmosphere Community
358 Climate Model Version 6, WACCM6) (72). We average together the gridded, monthly fields to produce
359 annual-mean fields, with each field having a grid resolution of 0.94240838 degrees latitude by 1.25
360 degrees longitude.

361
362 The ARISE data set includes two sets of simulations composed of ten ensemble members each. The first
363 set follows the SSP2-4.5 emissions scenario while the second is identical to the first but with the inclusion
364 of stratospheric aerosol injection (SAI) beginning in the year 2035. The location and amount of aerosols
365 released into the stratosphere each year is determined by a controller algorithm that works to keep global
366 mean temperature, the north-south temperature gradient, and the equator-to-pole temperature gradient at
367 values based on the 2020-2039 mean of the SSP2-4.5 simulations with CESM2 (WACCM6) (72). Further
368 details about the ARISE SAI configuration and aerosol injection strategy are provided in (50).

369
370 *Probability of perceived failure*

371 Decadal trends of annual mean temperature at each gridpoint are computed using linear, least-squares
372 regression over two ten-year periods: (1) the pre-deployment decade (2025-2034) and (2) the post-
373 deployment decade (2035-2044). Since SAI under ARISE is designed to stabilize global-mean
374 temperature (not to reverse the warming trend and induce cooling), we define “warming” as any decadal
375 trend that exceeds 0.1°C per decade. A warming threshold of 0.1°C per decade is chosen to reflect the
376 approximate warming we have thus far experienced over the observational record (NOAA National
377 Centers for Environmental Information, published online January 2021). All trend magnitudes less than
378 this are considered “not warming”. We thus classify each of the ensemble members, for each location, as
379 falling into one of the four archetypes of perceived success of climate intervention, based on the pre-
380 and/or post-deployment trends: 1) Rebound Warming (i.e. no warming followed by warming); 2)
381 Continued Warming (i.e. warming followed by more warming); 3) Stabilization (i.e. no warming either
382 before or after deployment); and, 4) Recovery (i.e. warming followed by no warming). The combination
383 of Rebound warming and Continued warming represent the experience of potential “perceived failure”, as
384 both exhibit warming trends over the post-deployment decade that exceed 0.1°C per decade. The
385 probability of perceived failure is then computed as the percent of ensemble members (out of 10) that
386 experience perceived failure at each location.

387
388 *Populations and country-level statistics for those experiencing perceived failure*

389 Projected, gridded population data for the year 2040 were downloaded from SEDAC for Shared
390 Socioeconomic Pathway 2 (SSP2) (
391 <https://sedac.ciesin.columbia.edu/data/collection/popdynamics/maps/services>). The SEDAC data was
392 downloaded in netcdf format at a resolution of one eighth of a degree and was then re-gridded to the
393 ARISE/CESM2 grid using the sum function. The global population is perfectly conserved in this
394 regridding process. The population experiencing perceived failure is then computed as the sum of the
395 populations at each gridpoint where the post-deployment decade exhibits warming trends greater than 0.1
396 °C. Projected gross domestic product (GDP; in units of purchasing power parity) data for the year 2040
397 under SSP2 were downloaded as shapefiles from IIASA at the country level
398 (<https://tntcat.iiasa.ac.at/SspDb/dsd?Action=htmlpage&page=10>). Temperature trends, projected
399 population, and projected GDP were then calculated within each country boundary using the python
400 packages *regionmask* and *geopandas*.

401

402 Fig. 4D includes the percent of members with 10% or more of a country's projected 2040 population
403 experiencing perceived failure following SAI deployment. Fig S5 displays results for the same analysis
404 using alternative population thresholds (i.e. 5%, 10%, 25% and 50%).

405

406 *Probability of exceeding pre-deployment maximum temperature*

407 For each gridpoint, we computed the maximum annual-mean temperature across all available years prior
408 to SAI deployment (2015-2034). This was done for each ensemble member separately to simulate
409 perceptions within each individual realization of the climate system. The probability of exceeding the pre-
410 deployment maximum temperature was then defined as the number of ensemble members (out of 10) that
411 exceeded their pre-deployment maximum in the decade following deployment (2035-2044).

412

413

414 **References**

- 415 1. IPCC, “Summary for Policymakers,” Masson-Delmotte, V., P. Zhai, A. Pirani, S.L. Connors, C.
416 Péan, S. Berger, N. Caud, Y. Chen, L. Goldfarb, M.I. Gomis, M. Huang, K. Leitzell, E. Lonnoy, J.B.R.
417 Matthews, T.K. Maycock, T. Waterfield, O. Yelekçi, R. Yu, and B. Zhou, Ed. (Intergovernmental Panel
418 on Climate Change, 2021).
- 419 2. UNEP, “Emissions gap report 2021: the heat is on—a world of climate promises not yet
420 delivered” (United Nations Environment Programme Nairobi, Kenya, 2021).
- 421 3. NASEM, *Negative Emissions Technologies and Reliable Sequestration: A Research Agenda*
422 (National Academies Press, 2019).
- 423 4. IPCC, “Summary for Policymakers” (Cambridge University Press, 2022).
- 424 5. K. S. Sheldon, Climate Change in the Tropics: Ecological and Evolutionary Responses at Low
425 Latitudes. *Annu. Rev. Ecol. Evol. Syst.* (2019) <https://doi.org/10.1146/annurev-ecolsys-110218-025005>
426 (May 24, 2022).
- 427 6. H. Hartmann, *et al.*, Climate Change Risks to Global Forest Health: Emergence of Unexpected
428 Events of Elevated Tree Mortality Worldwide. *Annu. Rev. Plant Biol.* **73**, 673–702 (2022).
- 429 7. F. V. Davenport, M. Burke, N. S. Diffenbaugh, Contribution of historical precipitation change to
430 US flood damages. *Proc. Natl. Acad. Sci. U. S. A.* **118** (2021).
- 431 8. N. S. Diffenbaugh, M. Burke, Global warming has increased global economic inequality. *Proc.*
432 *Natl. Acad. Sci. U. S. A.* **116**, 9808–9813 (2019).
- 433 9. T. Dietz, R. L. Shwom, C. T. Whitley, Climate Change and Society. *Annu. Rev. Sociol.* (2020)
434 <https://doi.org/10.1146/annurev-soc-121919-054614> (May 24, 2022).
- 435 10. T. M. Lenton, *et al.*, Climate tipping points - too risky to bet against. *Nature* **575**, 592–595
436 (2019).
- 437 11. N. Boers, M. Rypdal, Critical slowing down suggests that the western Greenland Ice Sheet is
438 close to a tipping point. *Proc. Natl. Acad. Sci. U. S. A.* **118** (2021).
- 439 12. J. Lohmann, P. D. Ditlevsen, Risk of tipping the overturning circulation due to increasing rates of
440 ice melt. *Proc. Natl. Acad. Sci. U. S. A.* **118** (2021).
- 441 13. S. H. R. Rosier, *et al.*, The tipping points and early warning indicators for Pine Island Glacier,
442 West Antarctica. *cryosphere* **15**, 1501–1516 (2021).
- 443 14. NASEM, *Reflecting Sunlight: Recommendations for Solar Geoengineering Research and*
444 *Research Governance* (National Academies Press, 2021).
- 445 15. D. W. Keith, Toward constructive disagreement about geoengineering. *Science* **374**, 812–815
446 (2021).

- 447 16. J. C. S. Long, J. G. Shepherd, “The Strategic Value of Geoengineering Research” in *Global*
448 *Environmental Change*, B. Freedman, Ed. (Springer Netherlands, 2014), pp. 757–770.
- 449 17. D. G. MacMartin, K. L. Ricke, D. W. Keith, Solar geoengineering as part of an overall strategy
450 for meeting the 1.5°C Paris target. *Philos. Trans. A Math. Phys. Eng. Sci.* **376** (2018).
- 451 18. A. Jones, *et al.*, The impact of abrupt suspension of solar radiation management (termination
452 effect) in experiment G2 of the Geoengineering Model Intercomparison Project (GeoMIP). *J. Geophys.*
453 *Res.* **118**, 9743–9752 (2013).
- 454 19. K. E. McCusker, K. C. Armour, C. M. Bitz, D. S. Battisti, Rapid and extensive warming
455 following cessation of solar radiation management. *Environ. Res. Lett.* **9**, 024005 (2014).
- 456 20. J. F. Tjiputra, A. Grini, H. Lee, Impact of idealized future stratospheric aerosol injection on the
457 large-scale ocean and land carbon cycles. *J. Geophys. Res. Biogeosci.* **121**, 2–27 (2016).
- 458 21. P. J. Irvine, B. Kravitz, M. G. Lawrence, H. Muri, An overview of the Earth system science of
459 solar geoengineering. *Wiley Interdiscip. Rev. Clim. Change* **7**, 815–833 (2016).
- 460 22. H. J. Buck, Geoengineering: re-making climate for profit or humanitarian intervention? *Dev.*
461 *Change* **43**, 253–270 (2012).
- 462 23. J. A. Flegal, A. Gupta, Evoking equity as a rationale for solar geoengineering research?
463 Scrutinizing emerging expert visions of equity. *International Environmental Agreements: Politics, Law*
464 *and Economics* **18**, 45–61 (2018).
- 465 24. A. Mahajan, D. Tingley, G. Wagner, Fast, cheap, and imperfect? US public opinion about solar
466 geoengineering. *Env. Polit.* **28**, 523–543 (2019).
- 467 25. D. G. MacMartin, P. J. Irvine, B. Kravitz, J. B. Horton, Technical characteristics of a solar
468 geoengineering deployment and implications for governance. *Clim. Policy* **19**, 1325–1339 (2019).
- 469 26. F. Fröb, S. Sonntag, J. Pongratz, H. Schmidt, T. Ilyina, Detectability of artificial ocean
470 alkalization and stratospheric aerosol injection in MPI-ESM. *Earths Future* **8** (2020).
- 471 27. N. S. Diffenbaugh, *et al.*, Quantifying the influence of global warming on unprecedented extreme
472 climate events. *Proc. Natl. Acad. Sci. U. S. A.* **114**, 4881–4886 (2017).
- 473 28. N. S. Diffenbaugh, D. L. Swain, D. Touma, Anthropogenic warming has increased drought risk in
474 California. *Proc. Natl. Acad. Sci. U. S. A.* **112**, 3931–3936 (2015).
- 475 29. T. Woollings, *et al.*, Daily to Decadal Modulation of Jet Variability. *J. Clim.* **31**, 1297–1314
476 (2018).
- 477 30. C. Deser, “certain uncertainty: The role of internal climate variability in projections of regional
478 climate change and risk management.” *Earths Future* **8** (2020).
- 479 31. Z. Labe, G. Magnusdottir, H. Stern, Variability of Arctic Sea Ice Thickness Using PIOMAS and
480 the CESM Large Ensemble. *J. Clim.* **31**, 3233–3247 (2018).

- 481 32. W. Cai, *et al.*, Changing El Niño–Southern Oscillation in a warming climate. *Nature Reviews*
482 *Earth & Environment* **2**, 628–644 (2021).
- 483 33. Z. Martin, *et al.*, The influence of the quasi-biennial oscillation on the Madden–Julian oscillation.
484 *Nature Reviews Earth & Environment* **2**, 477–489 (2021).
- 485 34. J. S. Mankin, F. Lehner, S. Coats, K. A. McKinnon, The value of initial condition large
486 ensembles to robust adaptation decision-making. *Earths Future* **8** (2020).
- 487 35. D. W. Keith, “Geoengineering the Climate: History and Prospect 1” in *The Ethics of*
488 *Nanotechnology, Geoengineering and Clean Energy*, (Routledge, 2020), pp. 207–246.
- 489 36. B. Kravitz, *et al.*, A multi-model assessment of regional climate disparities caused by solar
490 geoengineering. *Environ. Res. Lett.* **9**, 074013 (2014).
- 491 37. K. L. Ricke, M. G. Morgan, M. R. Allen, Regional climate response to solar-radiation
492 management. *Nat. Geosci.* **3**, 537–541 (2010).
- 493 38. G. A. Ban-Weiss, K. Caldeira, Geoengineering as an optimization problem. *Environ. Res. Lett.* **5**,
494 034009 (2010).
- 495 39. I. R. Simpson, *et al.*, The regional hydroclimate response to stratospheric sulfate geoengineering
496 and the role of stratospheric heating. *J. Geophys. Res.* **124**, 12587–12616 (2019).
- 497 40. A. Brügger, C. Demski, S. Capstick, How Personal Experience Affects Perception of and
498 Decisions Related to Climate Change: A Psychological View. *Weather, Climate, and Society* **13**, 397–408
499 (2021).
- 500 41. C. P. Borick, B. G. Rabe, “Personal experience, extreme weather events, and perceptions of
501 climate change” in *Oxford Research Encyclopedia of Climate Science*, (2017).
- 502 42. W. Shao, J. C. Garand, B. D. Keim, L. C. Hamilton, Science, scientists, and local weather:
503 Understanding mass perceptions of global warming. *Soc. Sci. Q.* **97**, 1023–1057 (2016).
- 504 43. A. Parker, P. J. Irvine, The risk of termination shock from solar geoengineering. *Earths Future* **6**,
505 456–467 (2018).
- 506 44. S. Baur, A. Nauels, C.-F. Schleussner, Deploying Solar Radiation Modification to limit warming
507 under a current climate policy scenario results in a multi-century commitment. *Earth System Dynamics*
508 *Discussions* (2022) <https://doi.org/10.5194/esd-2022-17>.
- 509 45. J. Garbe, T. Albrecht, A. Levermann, J. F. Donges, R. Winkelmann, The hysteresis of the
510 Antarctic Ice Sheet. *Nature* **585**, 538–544 (2020).
- 511 46. C. Mora, *et al.*, Global risk of deadly heat. *Nat. Clim. Chang.* **7**, 501–506 (2017).
- 512 47. K. L. Ricke, K. Caldeira, Natural climate variability and future climate policy. *Nat. Clim. Chang.*
513 **4**, 333–338 (2014).

- 514 48. C. Deser, A. Phillips, V. Bourdette, H. Teng, Uncertainty in climate change projections: the role
515 of internal variability. *Clim. Dyn.* **38**, 527–546 (2012).
- 516 49. B. Kravitz, *et al.*, The geoengineering model intercomparison project (GeoMIP). *Atmos. Sci. Lett.*
517 **12**, 162–167 (2011).
- 518 50. J. Richter, *et al.*, Assessing Responses and Impacts of Solar climate intervention on the Earth
519 system with stratospheric aerosol injection (ARISE-SAI). *EGUsphere*, 1–35 (2022).
- 520 51. J. E. Kay, C. Deser, A. Phillips, A. Mai, The Community Earth System Model (CESM) large
521 ensemble project: A community resource for studying climate change in the presence of internal climate
522 *Bulletin of the* (2015).
- 523 52. Y. Xu, V. Ramanathan, Well below 2 °C: Mitigation strategies for avoiding dangerous to
524 catastrophic climate changes. *PNAS* (2017) (May 19, 2022).
- 525 53. S. Milinski, N. Maher, D. Olonscheck, How large does a large ensemble need to be? *Earth*
526 *System Dynamics* **11**, 885–901 (2020).
- 527 54. NOAA National Centers for Environmental Information, “State of the Climate: Monthly Global
528 Climate Report for Annual 2020” (National Oceanographic and Atmospheric Administration, published
529 online January 2021).
- 530 55. E. Rignot, J. Mouginot, B. Scheuchl, Four decades of Antarctic Ice Sheet mass balance from
531 1979–2017. *Proceedings of the* (2019).
- 532 56. A. Capotondi, C. Deser, A. S. Phillips, Y. Okumura, S. M. Larson, ENSO and pacific decadal
533 variability in the community earth system model version 2. *J. Adv. Model. Earth Syst.* **12** (2020).
- 534 57. M. J. Mills, *et al.*, Radiative and chemical response to interactive stratospheric sulfate aerosols in
535 fully coupled CESM1(WACCM). *J. Geophys. Res.* **122**, 13,061–13,078 (2017).
- 536 58. K. L. Ebi, *et al.*, Extreme Weather and Climate Change: Population Health and Health System
537 Implications. *Annu. Rev. Public Health* **42**, 293–315 (2021).
- 538 59. J. Gao, “Downscaling Global Spatial Population Projections from 1/8-degree to 1-km Grid Cells”
539 (National Center for Atmospheric Research, 2017) <https://doi.org/10.5065/D60Z721H>.
- 540 60. J. Gao, Global 1-km Downscaled Population Base Year and Projection Grids Based on the Shared
541 Socioeconomic Pathways, Revision 01 (2020) <https://doi.org/10.7927/q7z9-9r69>.
- 542 61. O. Renn, The social amplification/attenuation of risk framework: application to climate change.
543 *Wiley Interdiscip. Rev. Clim. Change* **2**, 154–169 (2011).
- 544 62. K. Sambrook, E. Konstantinidis, S. Russell, Y. Okan, The Role of Personal Experience and Prior
545 Beliefs in Shaping Climate Change Perceptions: A Narrative Review. *Front. Psychol.* **12**, 669911 (2021).
- 546 63. J. Crespo Cuaresma, Income projections for climate change research: A framework based on
547 human capital dynamics. *Glob. Environ. Change* **42**, 226–236 (2017).

- 548 64. W. Smith, G. Wagner, Stratospheric aerosol injection tactics and costs in the first 15 years of
549 deployment. *Environ. Res. Lett.* **13**, 124001 (2018).
- 550 65. National Research Council, National Research Council (U.S.). Division on Earth and Life
551 Studies, National Research Council (U.S.). Ocean Studies Board, National Research Council (U.S.).
552 Board on Atmospheric Sciences and Climate, Committee on Geoengineering Climate: Technical
553 Evaluation and Discussion of Impacts, *Climate Intervention: Reflecting Sunlight to Cool Earth* (National
554 Academies Press, 2015).
- 555 66. IPCC, “Climate Change 2022: Mitigation of Climate Change. Contribution of Working Group III
556 to the Sixth Assessment Report of the Intergovernmental Panel on Climate Change” (Cambridge
557 University Press, 2022) <https://doi.org/10.1017/9781009157926>.
- 558 67. N. S. Diffenbaugh, E. Barnes, P. Keys, Probability of continued local-scale warming and extreme
559 events during and after decarbonization (2022).
- 560 68. S. Lewandowsky, L. Whitmarsh, Climate communication for biologists: When a picture can tell a
561 thousand words. *PLoS Biol.* **16**, e2006004 (2018).
- 562 69. M. Newman, M. A. Alexander, T. R. Ault, The Pacific Decadal Oscillation, Revisited. *J. Clim.*
563 **29**, 4399–4427 (2016).
- 564 70. S. Fankhauser, *et al.*, The meaning of net zero and how to get it right. *Nat. Clim. Chang.* **12**, 15–
565 21 (2021).
- 566 71. G. Danabasoglu, *et al.*, The community earth system model version 2 (CESM2). *J. Adv. Model.*
567 *Earth Syst.* **12** (2020).
- 568 72. G. A. Meehl, *et al.*, Characteristics of future warmer base states in CESM2. *Earth Space Sci.* **7**
569 (2020).
- 570 73. S. Tilmes, *et al.*, CESM1(WACCM) Stratospheric Aerosol Geoengineering Large Ensemble
571 Project. *Bull. Am. Meteorol. Soc.* **99**, 2361–2371 (2018).
- 572

573
574
575
576
577
578
579
580
581
582
583
584
585
586
587
588
589
590
591
592
593
594
595
596
597
598
599

Supplementary Information for

**Potential for Perceived Failure of Stratospheric Aerosol
Injection Deployment**

Patrick W. Keys^{1,2*}, Elizabeth A. Barnes¹, Noah S. Diffenbaugh³, James W. Hurrell¹ and Curtis M. Bell⁴

¹ Department of Atmospheric Science, Colorado State University

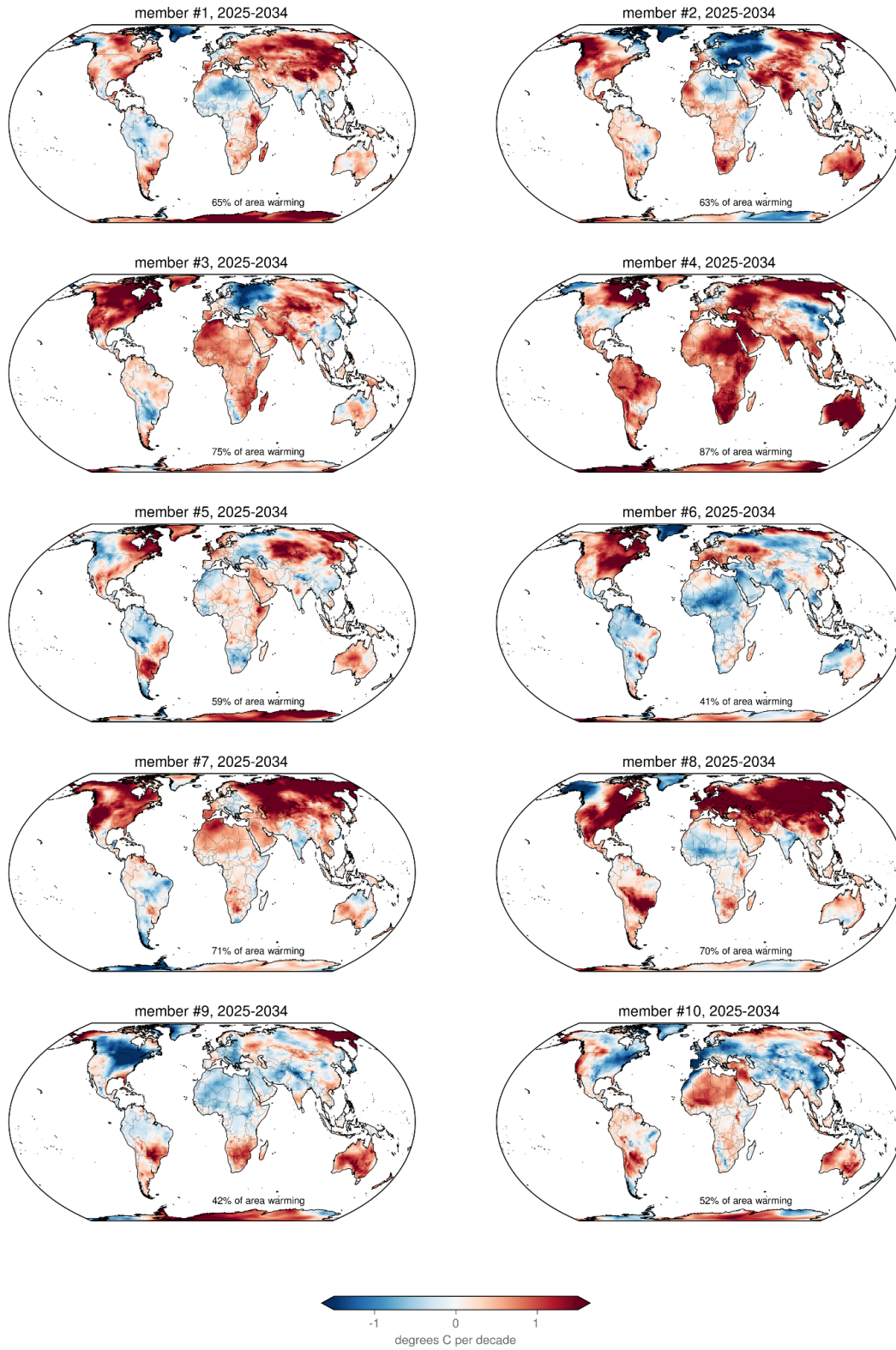
² School of Global Environmental Sustainability, Colorado State University

³ Doerr School of Sustainability, Stanford University

⁴ International Programs Department, United States Naval War College

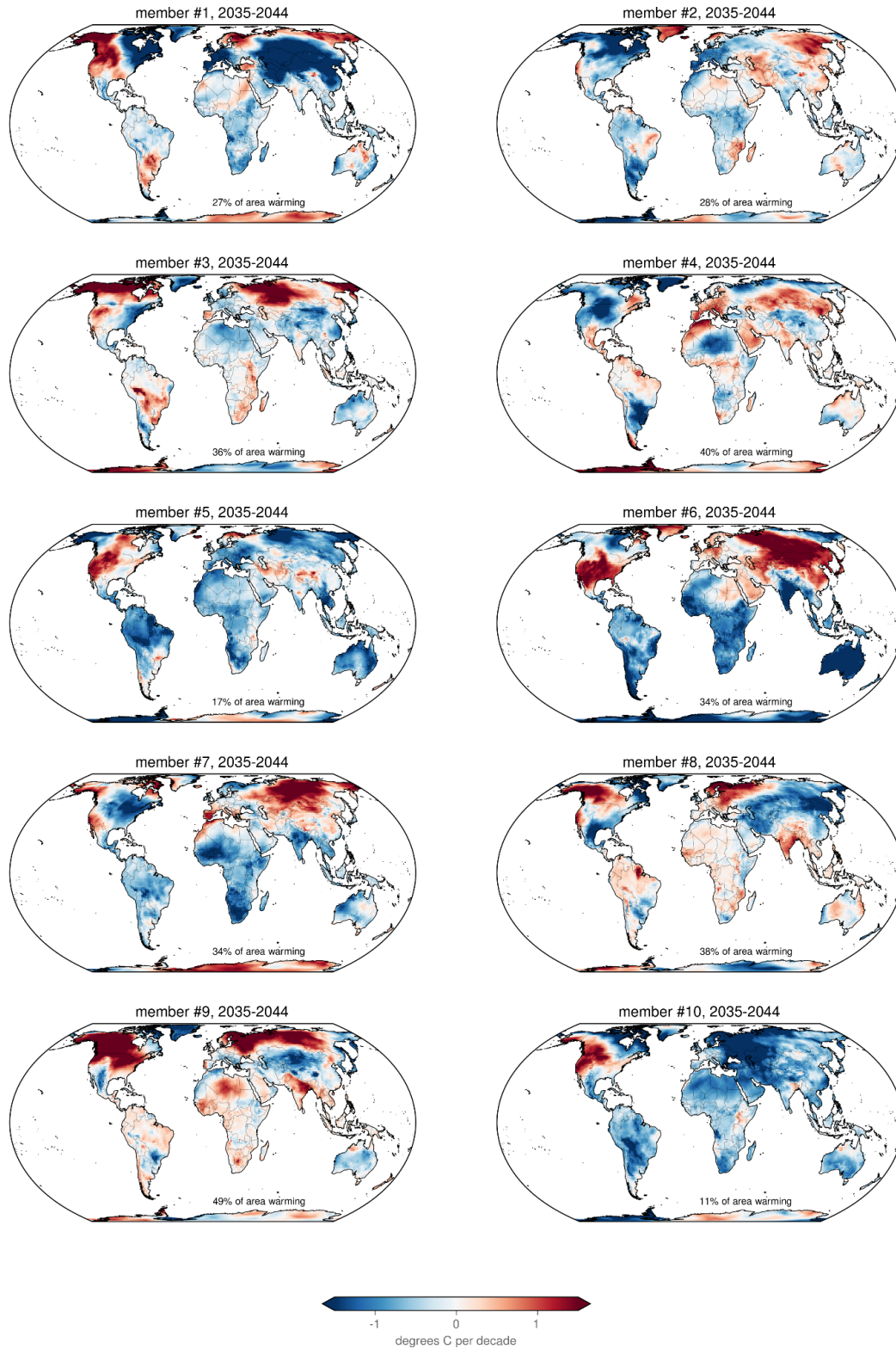
***Corresponding Author:** Patrick W. Keys

Email: patrick.keys@colostate.edu



600

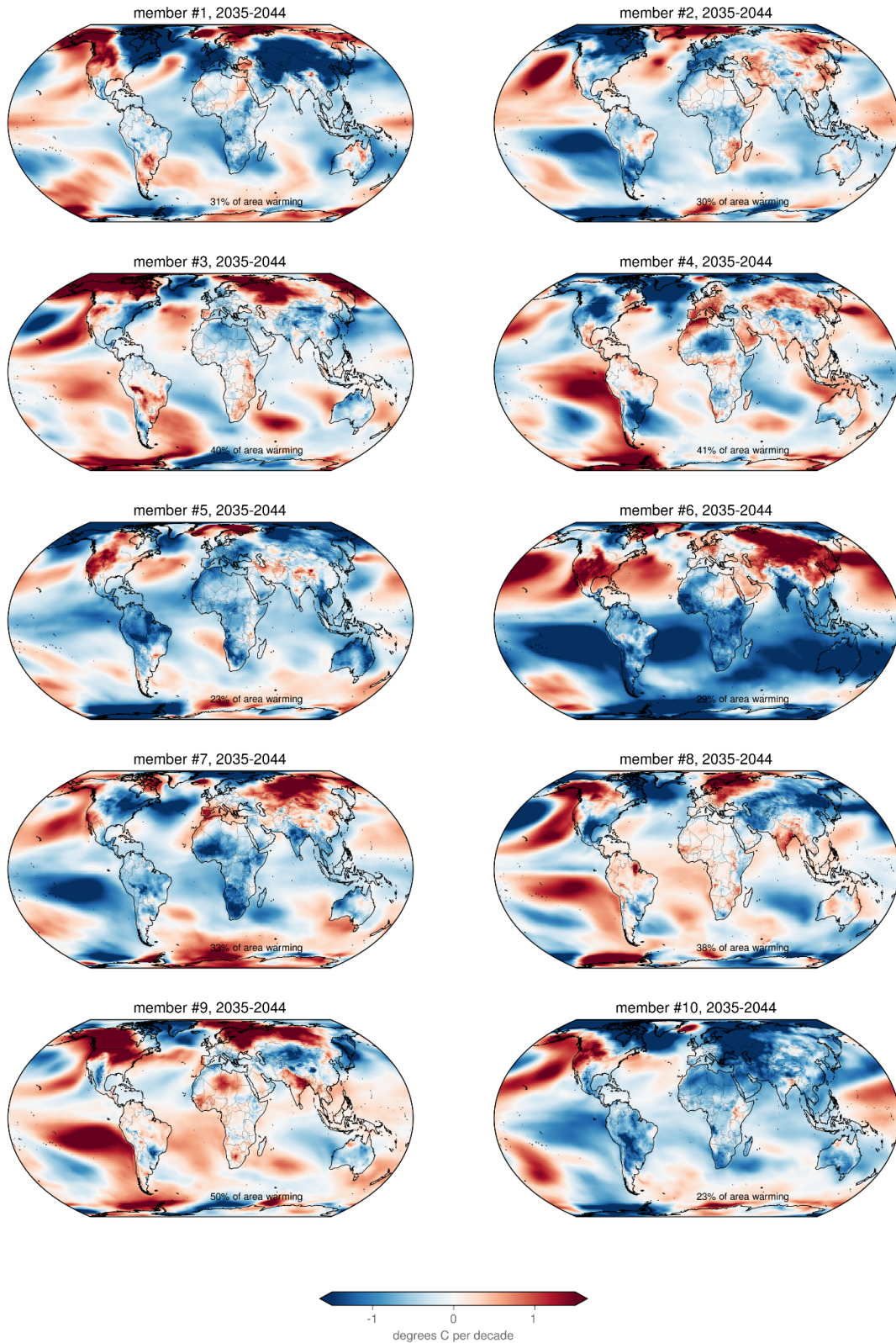
601 Fig. S1. As in Figure 1D but for all 10 ensemble members.



602

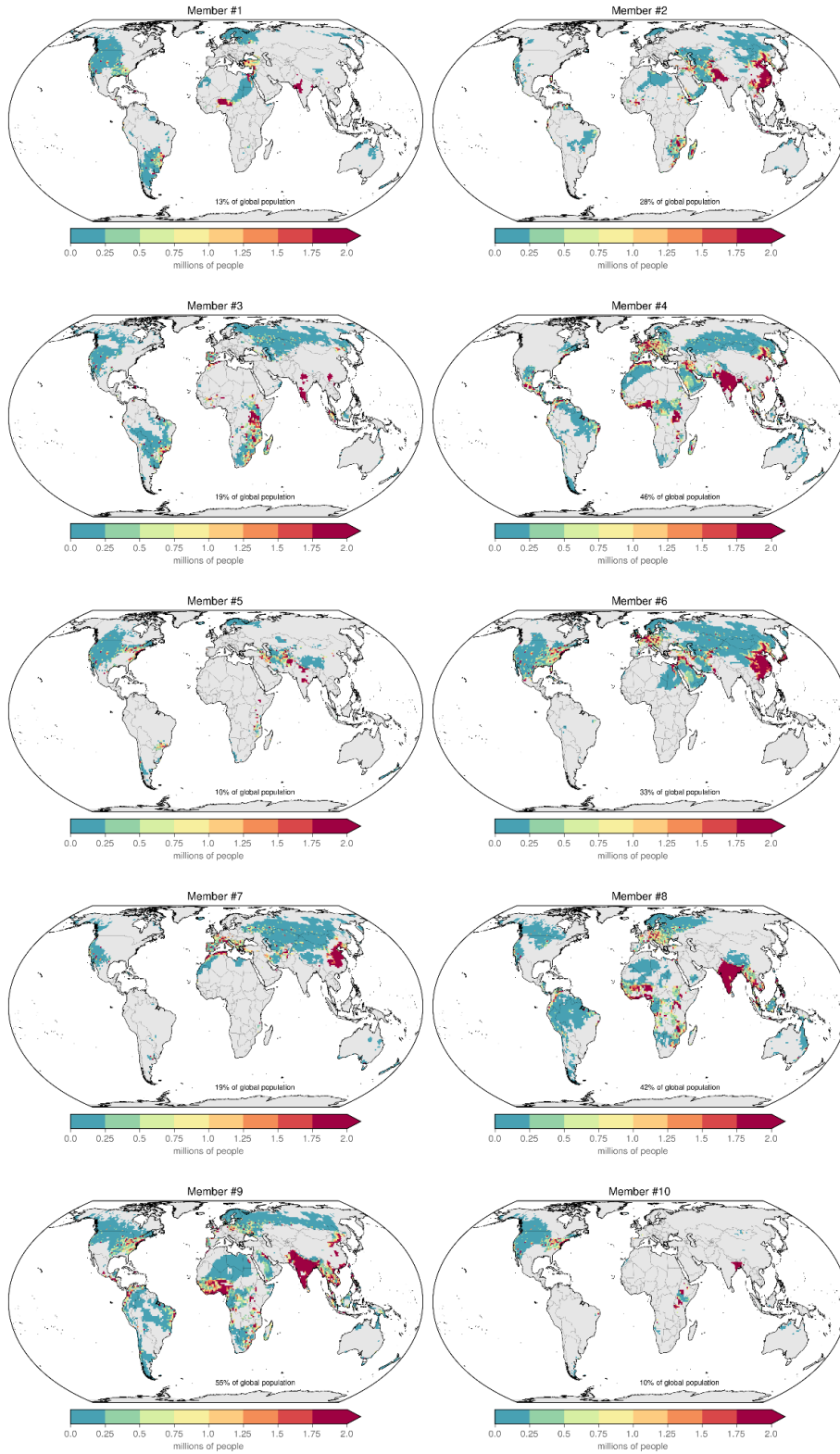
603 Fig. S2. As in Figure 1E but for all 10 ensemble members.

604



605

606 Fig. S3. As in Fig. S2 but including temperatures over the oceans.



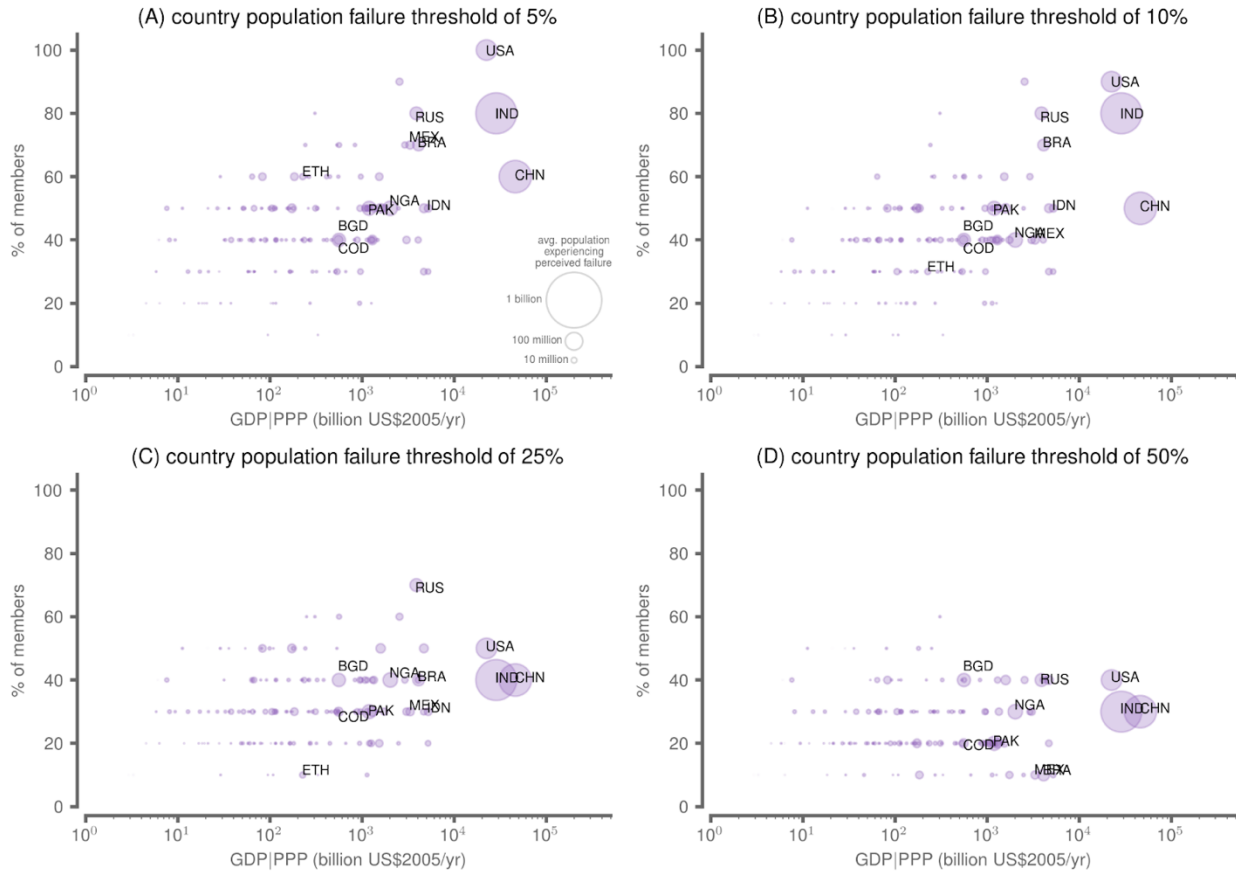
607

608 Fig. S4. As in Fig. 4A but for all 10 ensemble members.

609

610

Countries experiencing perceived failure



611

612

613 **Fig. S5.** As in Fig. 4B but for different population failure thresholds. The 10% threshold shown here in panel (B) is

614 what is displayed in the main text.

615

616 **Supplemental Methods**

617

618 *GLENS Data*

619 Gridded, monthly near surface air temperature fields (variable name TREFHT) were obtained from the ensemble of
620 simulations performed for the Stratospheric Aerosol Geoengineering Large Ensemble (GLENS-SAI) project (73).

621 The GLENS-SAI ensemble was simulated with the Community Earth System Model, version 1, as described in (57).

622 We average together the gridded, monthly fields to produce annual-mean fields, with each field having a grid
623 resolution of 0.9 degrees latitude by 1.25 degrees longitude.

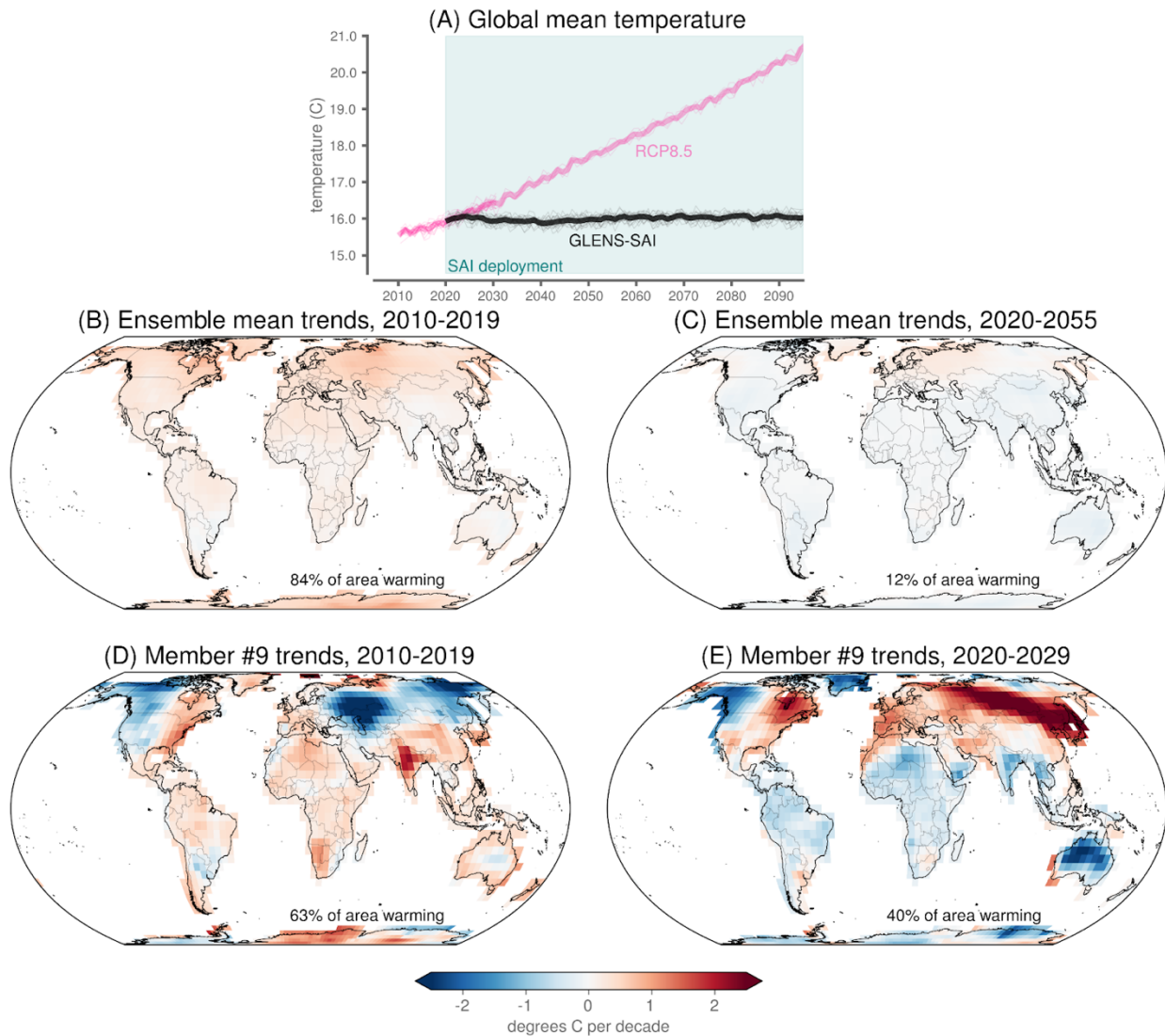
624

625 The GLENS-SAI data set includes two sets of simulations composed of twenty one ensemble members each. The
626 first set follows the RCP8.5 emissions scenario while the second is identical to the first but with the inclusion of
627 stratospheric aerosol injection (SAI) beginning in the year 2020. The location and amount of aerosols released into
628 the stratosphere each year is determined by a controller algorithm that works to keep global mean temperature, the
629 north-south temperature gradient, and the equator-to-pole temperature gradient at values based 2020. The 2020
630 mean conditions are calculated based on the first 13 members of the RCP8.5 scenario simulations. Further details
631 about the GLENS-SAI configuration and aerosol injection strategy are provided in (73).

632

633 *Probability of perceived failure*

634 Decadal trends of annual mean temperature at each gridpoint are computed using linear, least-squares regression
635 over two ten-year periods: (1) the pre-deployment decade (2010-2019) and (2) the post-deployment decade (2020-
636 2029). Since SAI under GLENS is designed to stabilize global-mean temperature (not to reverse the warming trend
637 and induce cooling), we define “warming” as any decadal trend that exceeds 0.1°C per decade. A warming threshold
638 of 0.1°C per decade is chosen to reflect the approximate warming we have thus far experienced over the
639 observational record (NOAA National Centers for Environmental Information, published online January 2021). All
640 trend magnitudes less than this are considered “not warming”. We thus classify each of the ensemble members, for
641 each location, as falling into one of the four archetypes of perceived success of climate intervention, based on the
642 pre- and/or post-deployment trends: 1) Rebound Warming (i.e. no warming followed by warming); 2) Continued
643 Warming (i.e. warming followed by more warming); 3) Stabilization (i.e. no warming either before or after
644 deployment); and, 4) Recovery (i.e. warming followed by no warming). The combination of Rebound warming and
645 Continued warming represent the experience of potential “perceived failure”, as both exhibit warming trends over
646 the post-deployment decade that exceed 0.1°C per decade. The probability of perceived failure is then computed as
647 the percent of ensemble members (out of 20) that experience perceived failure at each location.

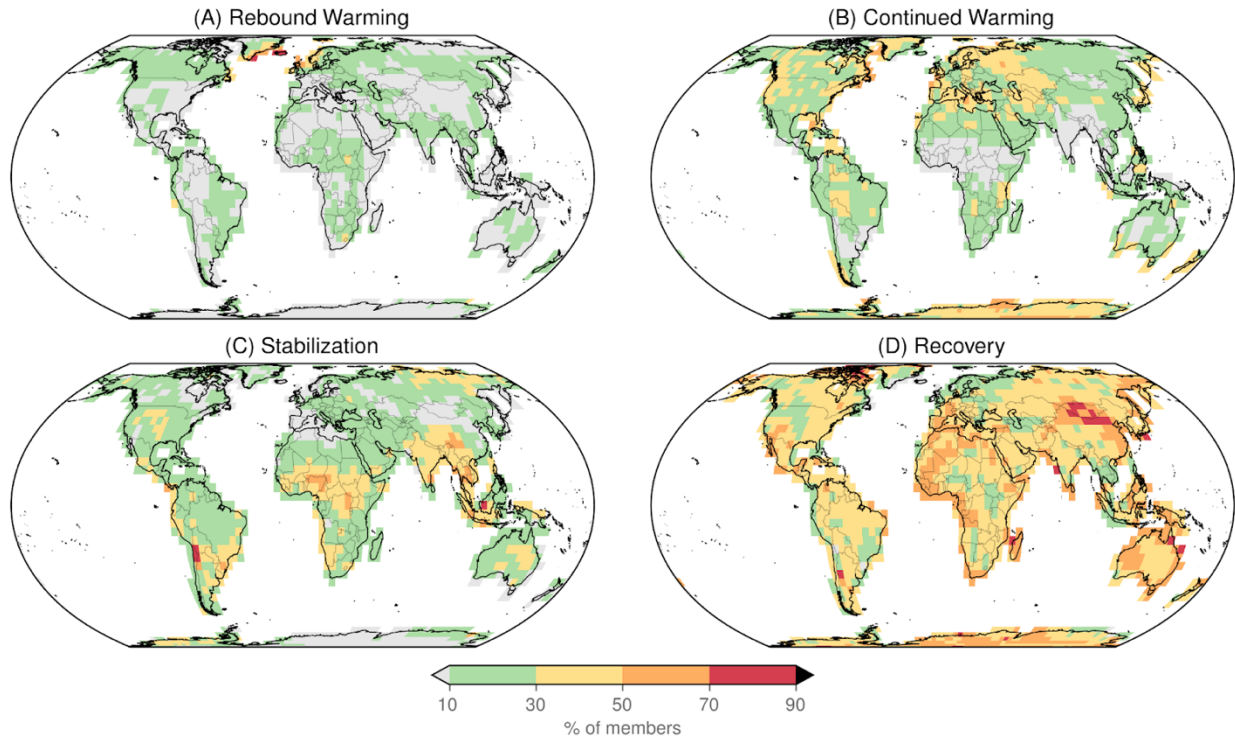


649

650 **Figure S6. Surface temperature trends.** (A) Global mean surface temperature. Gray lines denote individual
 651 ensemble members and the black line denotes the ensemble mean. (B,C) Ensemble-mean trends over (B) 2010-2019
 652 under RCP8.5 and (C) 2020-2055 with GLENS SAI deployment. (D,E) Trends over the (D) pre-deployment decade
 653 and (E) post-deployment decade for ensemble member #9. (B-D) The percentage in the bottom of the maps denotes
 654 the percentage of land area that exhibits warming trends as defined in the text. Similar figure as in Figure 1 of the
 655 Main text.

656

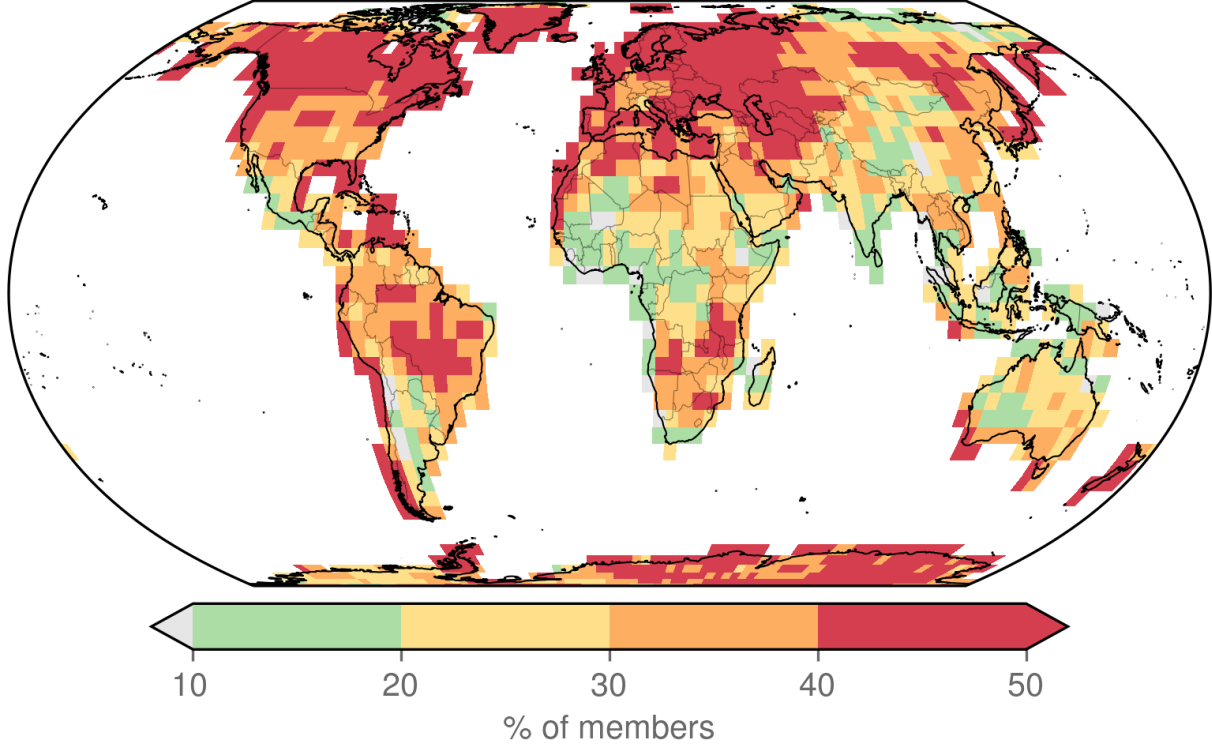
657



658
 659
 660
 661
 662
 663

Figure S7. Archetypal regional responses to GLENS-SAI. The percent of ensemble members that exhibit specific archetypal responses over the ten years pre- and post-deployment: **(A)** Rebound Warming (not warming followed by warming), **(B)** Continued Warming (warming followed by warming), **(C)** Stabilization (not warming followed by not warming) and **(D)** Recovery (warming followed by not warming). Similar figure as in Figure 3 in the Main text.

GLENS Probability of perceived failure (2020-2029)



664

665 **Figure S7. Probability of perceived failure under GLENS-SAI over the post-deployment period,** where the
666 probability is computed as the fraction of ensemble members exhibiting warming trends (similar to Figure 4A in the
667 Main text).

668

669